J. Fluid Mech. (1972), *vol.* 52, *part* 4, *pp.* 657–682
Printed in Great Britain

A parametric study of self-similar blast waves

By A. K. OPPENHEIM, A. L. KUHL,
E. A. LUNDSTROM AND M. M. KAMEL
University of California, Berkeley

(Received 16 July 1971 and in revised form 3 January 1972)

The paper presents a comprehensive examination of self-similar blast waves with respect to two parameters, one describing the front velocity and the other the variation of the ambient density immediately ahead of the front. All possible front trajectories are taken into account, including limiting cases of the exponential and logarithmic form. The structure of the waves is analysed by means of a phase plane defined in terms of two reduced co-ordinates $F \equiv (t/r\mu)\,u$ and $Z \equiv [(t/r\mu)\,a]^2$, where t and r are the independent (time and space) variables, $\mu \equiv d\ln r_n/d\ln t_n$, the subscript n denoting the co-ordinates of the front, and u and a are, respectively, the particle velocity and the speed of sound. Loci of extrema of the integral curves in the phase plane are traced and loci of singularities are determined on the basis of their intersections. Boundary conditions are introduced for the case when the medium into which the waves propagate is at rest. Representative solutions, pertaining to all the possible cases of blast waves bounded by shock fronts propagating into an atmosphere of uniform density, are obtained by evaluating the integral curves and determining the corresponding profiles of the gasdynamic parameters. Particular examples of integral curves for waves bounded by detonations are given and all the degenerate solutions, corresponding to cases where the integral curve is reduced to a point, are delineated.

1. Introduction

The concept of self-similarity has played a key role in the development of blast-wave theory. There were, of course, some good reasons for this: basic studies in this field were prompted by the interest in strong explosions, notably those due to atom bombs, and self-similar solutions apply particularly well to such cases; the concept of self-similarity results directly from dimensional analysis, the obvious first step in treating a new class of physical problems, and it yields most readily information on the salient properties of the phenomena under study, an obvious objective for an initial investigation. Thus the postulate of self-similarity formed the basis for all the classical papers (Von Neumann 1941; Taylor 1941; Sedov 1945), all the early studies (Taylor 1946; Sedov 1946; Stanyukovich 1946) and all the texts in this field (Courant & Friedrichs 1948; Sedov 1957; Stanyukovich 1955; Korobeinikov *et al.* 1961; Zel'dovich & Raizer 1966). Using this formulation, a great variety of problems, concerning both explosions and implosions, were treated by many investigators (Krasheninnikova

1955; Grodzovskii 1956; Rogers 1958; Grigorian 1958*a*, *b*; Kochina & Mel'nikova 1960) with the majority of publications being in the Soviet literature. A notable exception in this respect is the classical paper, on the self-similar strong free implosion, of Guderley (1942), followed by refinements contributed by Butler (1954), Bruslinskii & Kazdan (1963) and by Lee (1967).

It is important to note that all these investigations were restricted to the consideration of purely inertial effects, so that the medium was assumed to be essentially inviscid and behave as a perfect gas with constant specific heats, while the flow field was considered to be adiabatic. The purpose of this paper is to give a synthetic view of such self-similar flow fields with the above restrictions, but with a particular emphasis given to the physical meaning of the theory. In this connexion we present here salient properties of solutions depending on the values of two physically significant parameters: one describing the motion of the front and the other the variation in the ambient density of the medium into which the wave propagates.

2. Co-ordinates and parameters

In contrast to the conventional approach based on the dimensional analysis, the concept of self-similarity is treated here as a consequence of the reduction of partial differential equations expressing the conservation principles for blast waves to ordinary differential equations. Blast-wave equations in their general form were given in our earlier paper (Oppenheim *et al.* 1971), where they were formulated with respect to three fundamental systems of co-ordinates: the Eulerian space, Eulerian time and Lagrangian time systems.

The independent variables were expressed for this purpose in terms of the appropriate field co-ordinates

$$x \equiv r/r_n, \quad \tau \equiv t/t_n \tag{1}$$

and front co-ordinates

$$\xi \equiv r_n/r_0, \quad \eta \equiv t_n/t_0, \tag{2}$$

where r and t are the physical space and time variables, the subscript n refers to an arbitrary point on the trajectory of the front and the subscript 0 denotes a fixed reference point on this trajectory. Both explosions and implosions are included, as illustrated in figure 1. Here ϕ denotes lines of constant field co-ordinates† and π the particle path; as a consequence of the definitions in (1) the front of the wave corresponds to $\phi = 1$, while the piston trajectory is given by a particular value of $\phi = \phi_p$ which coincides with a particle path starting at the centre for explosions or at infinity for implosions. The Eulerian space profiles are referred to the abscissa $t = t_n$ (i.e. $\tau = 1$), the Eulerian time profiles are taken along the ordinate $r = r_n$ (i.e. $x = 1$) and the Lagrangian time profiles describe the variation of the gasdynamic parameters as a function of time along the particle path π.

† In this paper this becomes, in fact, the self-similarity variable $\phi \equiv x/\tau^{\mu}$, where μ is the velocity index defined in equation (5).

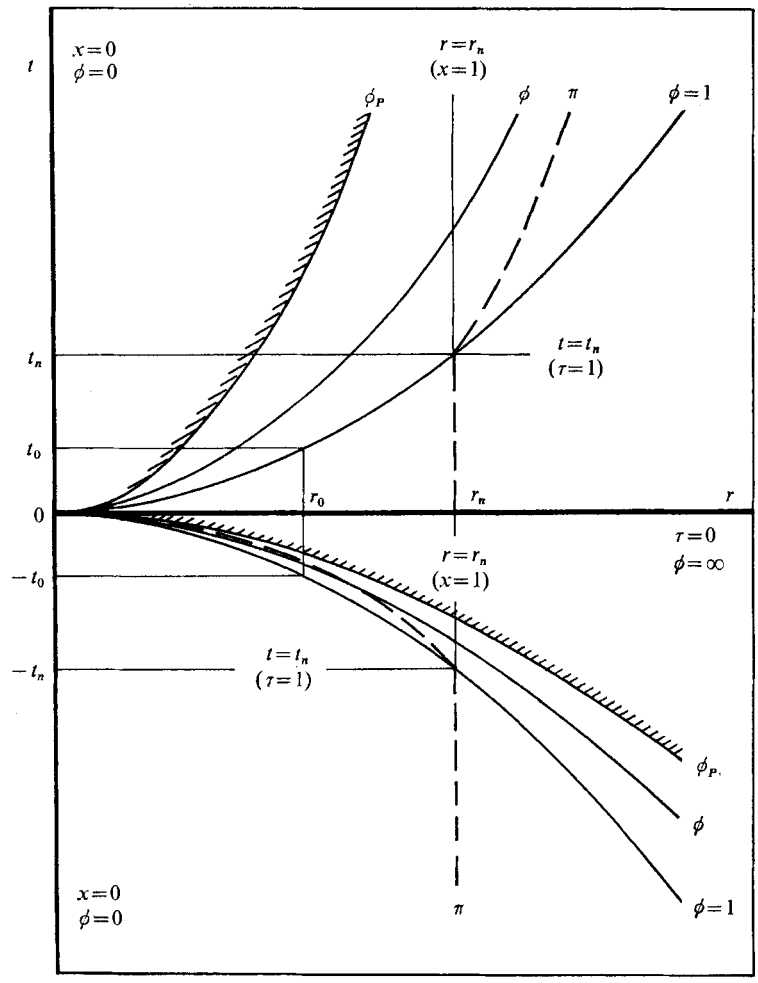

FIGURE 1. Blast-wave co-ordinates for explosions and implosions.

The reduction to ordinary differential equations is accomplished here by demanding that the flow field contains no sources and by annihilating the dependence on the front co-ordinates, defined by (2). Since, in the absence of sources, blast-wave equations are essentially autonomous in ϕ, in order to satisfy this requirement it is sufficient to eliminate all the terms containing partial derivatives with respect to the front co-ordinate, while the total derivatives with respect to this co-ordinate can be retained only if they are constant.

By observing that, by definition, the front of the blast wave is a gasdynamic discontinuity, we see that the only way its motion can affect the flow field is by the variation in its velocity of propagation w_n or in the Mach number M_n. Thus, if the velocity of sound in the ambient atmosphere is constant, this property is appropriately simulated by expressing the partial derivatives with respect to

the front co-ordinate in terms of the transformation

$$\frac{\partial}{\partial \ln \xi} = \lambda y \frac{\partial}{\partial y},$$

where $y \equiv M_n^{-2}$ and

$$\lambda \equiv -2\frac{d\ln w_n}{d\ln r_n} = \frac{d\ln y}{d\ln \xi}, \tag{3}$$

the latter being usually referred to as the decay parameter.

In the blast-wave equations expressed in terms of the Eulerian space co-ordinates the only other term involving the total derivative is

$$\omega \equiv -d\ln \rho_a / d\ln \xi, \tag{4}$$

where ρ_a is the ambient density immediately ahead of the front.

Thus, conservation equations for blast waves are reduced to ordinary differential equations if, in the case of flow without sources and a constant velocity of sound in the ambient atmosphere, one has either (i) $y = 0$, $\lambda =$ constant and thus variable front velocity corresponding to the so-called zero counterpressure or cold atmosphere condition, or (ii) $\lambda = 0$, that is, constant front velocity and hence $y =$ constant. Under the above restrictions, the variation of ambient density can be taken into account in both cases provided that, with reference to (4), $\omega =$ constant.

Conventionally, for self-similar blast waves the motion of the front is expressed in terms of the velocity index

$$\mu \equiv \frac{d\ln \xi}{d\ln \eta} = \frac{d\ln r_n}{d\ln t_n} = \frac{t_n}{r_n} w_n. \tag{5}$$

This parameter is related to λ. Note that (3) can be transformed as follows:

$$\frac{\lambda}{2} = -\frac{d\ln (w_n/w_0)}{d\ln \xi} = -\frac{d}{d\ln \xi} \ln\left(\frac{\xi}{\eta}\frac{\mu}{\mu_0}\right), \tag{6}$$

where $\mu_0 = \mu$ at $\xi = \eta = 1$, hence

$$\frac{d\ln \mu}{d\ln \xi} = \frac{1}{\mu} - \frac{\lambda}{2} - 1. \tag{7}$$

The conventional form of self-similar blast waves, as obtained directly from the dimensional analysis, is associated with the condition of $\mu =$ constant. From (7) it follows that in this case $\lambda =$ constant, corresponding to the aforementioned condition (i). In this case the front trajectory in the time–space domain can be determined immediately from (5), which yields simply

$$\xi = \eta^{\mu}. \tag{8}$$

Self-similar blast waves associated with $\mu =$ constant cover, of course, most of the practical applications. There are, however, two interesting exceptions which correspond to $\lambda = -2$ and $\lambda = \infty$, when the blast-wave equations can acquire less conventional, limiting forms, first observed by Grigorian (1958*b*).

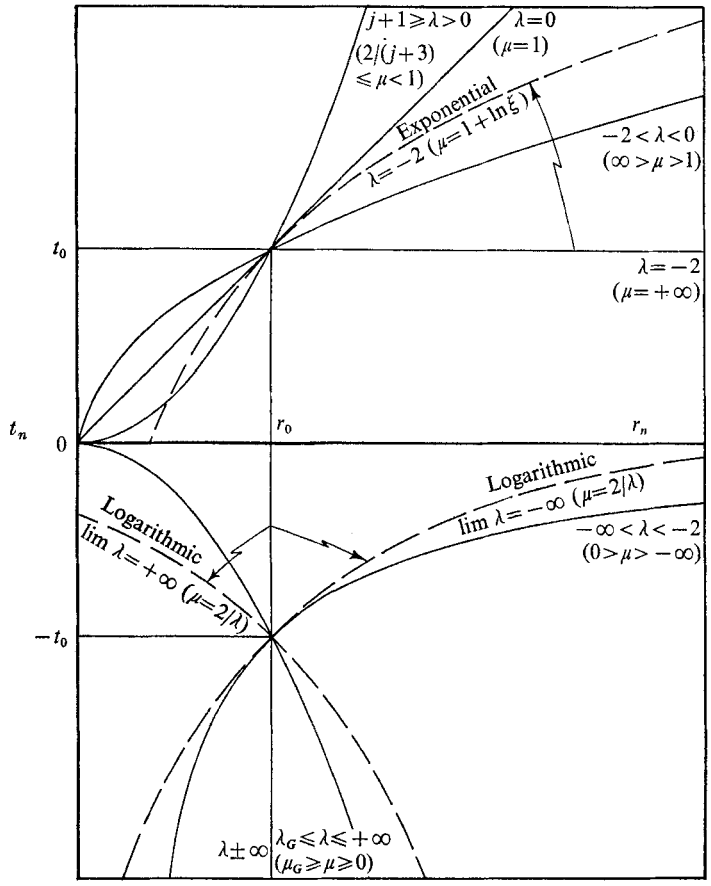

FIGURE 2. Front trajectories in the time–space domain. Broken lines depict the limiting cases of exponential and logarithmic trajectories.

The condition $\lambda = -2$ yields, in the case $\mu =$ constant, $\mu = \infty$. One can, however, obtain a limiting form for self-similar blast waves for this value of λ by allowing μ to be variable. Equation (7) then becomes

$$d \ln \mu / d \ln \xi = 1/\mu, \tag{9}$$

whence

$$\mu = \mu_0 + \ln \xi \tag{10}$$

and, by virtue of (5), the front trajectory is described by the exponential

$$\xi = \exp [\mu_0 (\eta - 1)]. \tag{11}$$

The condition of $\lambda = \infty$ corresponds, in the case of $\mu =$ constant, to $\mu = 0$. Now, however, λ can be eliminated from (7) by letting $\lambda = 2/\mu$. At the same time, as it will be demonstrated later,† λ is also eliminated from all the governing equations. In such circumstances (7) yields

$$d \ln \mu / d \ln \xi = -1, \tag{12}$$

whence

$$\mu = \mu_0 / \xi \tag{13}$$

† See equations (25*a*), (26*a*) and (28*a*).

and from (5) one obtains the logarithmic expression

$$\xi = 1 + \mu_0 \ln \eta \tag{14}$$

for the front trajectory. In fact it is this limiting case that was exploited for the treatment of blast waves in exponential atmospheres, as described by Zel'dovich & Raizer (1966) and subsequently refined by Hayes (1968).

The parametric study presented here covers all possible values of λ and μ for the case when the medium into which the blast wave propagates is at rest. Representative cases of front trajectories considered under such circumstances are shown in figure. 2. The conventional cases associated with μ = constant are represented by continuous lines, while the two limiting cases are demonstrated by broken lines and correspond to the particular value $\mu_0 = 1$.

3. Governing equations

By restricting the scope of the theory to gases with constant specific heat ratios γ, so that

$$\Gamma \equiv \rho a^2/p = \gamma = \text{constant}, \tag{15}$$

the most concise form of blast-wave equations is obtained, as demonstrated by Oppenheim *et al.* (1971), by using the reduced variables

$$F \equiv \frac{t}{r\mu} u, \quad Z \equiv \left(\frac{t}{r\mu} a\right)^2, \tag{16}$$

where u is the particle velocity and a is the local velocity of sound.†

Moreover, as a consequence of the restrictions imposed by the self-similarity requirements discussed in the previous section, blast-wave equations for all the three fundamental systems of co-ordinates considered in our previous paper (Oppenheim *et al.* 1971) can be expressed in terms of a single set by the introduction of the self-similar variable

$$\phi \equiv x/\tau^{\mu}, \tag{17}$$

reflecting the fact that, as it is apparent from dimensional considerations, a self-similar flow field in one co-ordinate system is self-similar in any other system. The transformation formulae for this purpose are

$$\frac{d}{d\ln\phi} = \frac{d}{d\ln x} = -\frac{1}{\mu}\frac{d}{d\ln\tau} = -\frac{1}{(1-F)\mu}\frac{d}{d\ln\tau} \tag{18}$$

for the Eulerian space, Eulerian time, and Lagrangian time systems respectively. The basis for the first two is straightforward; we use the relation $\tau = 1$ for the first and $x = 1$ for the second. The third, however, also involves the use of the kinematic relation expressing the fact that the particle velocity is the slope of the line of constant Lagrangian co-ordinate in the time–space domain.

In the limiting case of an exponential front trajectory ($\lambda = -2$) the equation of the trajectory of a constant field co-ordinate has the form of equation (11).

† It should be noted that for convenience the parameter Z is defined here so that it is γ times larger than the parameter Z of Oppenheim *et al.* (1971).

The solution is obtained here first in terms of Eulerian space profiles, the transformation to time profiles being given by the relation

$$\tau = 1 - \frac{1}{\mu_0} \ln x. \tag{19}$$

In the limiting case of a logarithmic front trajectory ($\lambda = \infty$) the equation of the trajectory of a constant field co-ordinate has the form of equation (14). In this case the solution is obtained first in terms of Eulerian time profiles, the transformation to space profiles being obtained by using the relation

$$x = 1 - \mu_0 \ln \tau. \tag{20}$$

In such circumstances the fundamental equations for self-similar blast waves can be expressed in terms of the following autonomous forms:

$$\frac{dF}{d\ln\phi} = -\frac{Q(F,Z)}{D(F,Z)} \tag{21}$$

and

$$\frac{dZ}{d\ln\phi} = -\frac{Z}{1-F}\frac{P(F,Z)}{D(F,Z)}, \tag{22}$$

whence

$$\frac{dZ}{dF} = \frac{Z}{1-F}\frac{P(F,Z)}{Q(F,Z)}. \tag{23}$$

Here,

$$D(F,Z) \equiv Z - (1-F)^2, \tag{24}$$

$$Q(F,Z) \equiv (j+1)(F-b)Z - (a-F)(1-F)F, \tag{25}$$

$$P(F,Z) \equiv \alpha(c-F)D(F,Z) + (\gamma-1)Q(F,Z), \tag{26}$$

with

$$\left.\begin{aligned} a \equiv \tfrac{1}{2}(\lambda+2), \quad b \equiv (\lambda+\omega)/(j+1)\gamma, \quad c \equiv (\lambda+2)/\alpha, \\ \alpha \equiv (j+1)(\gamma-1)+2 \end{aligned}\right\} \tag{27}$$

and $j = 0, 1, 2$ for plane, line and point symmetrical flow fields respectively.†

In order to explore the behaviour of solutions at $Z = \infty$ it is convenient to introduce $\hat{Z} \equiv Z^{-1}$, in terms of which (21), (22) and (23) become

$$\frac{dF}{d\ln\phi} = -\frac{\hat{Q}(F,\hat{Z})}{\hat{D}(F,\hat{Z})}, \tag{21a}$$

$$\frac{d\hat{Z}}{d\ln\phi} = +\frac{\hat{Z}}{1-F}\frac{\hat{P}(F,\hat{Z})}{\hat{D}(F,\hat{Z})}, \tag{22a}$$

$$\frac{d\hat{Z}}{dF} = -\frac{\hat{Z}}{1-F}\frac{\hat{P}(F,\hat{Z})}{\hat{Q}(F,\hat{Z})}, \tag{23a}$$

while (24), (25) and (26) become, respectively,

$$\hat{D}(F,\hat{Z}) = \hat{Z}D(F,Z) = 1 - \hat{Z}(1-F)^2, \tag{24a}$$

$$\hat{Q}(F,\hat{Z}) = \hat{Z}Q(F,Z) = (j+1)(F-b) - \hat{Z}(a-F)(1-F)F, \tag{25a}$$

$$\hat{P}(F,\hat{Z}) = \hat{Z}P(F,Z) = \alpha(c-F)\hat{D}(F,\hat{Z}) + (\gamma-1)\hat{Q}(F,\hat{Z}). \tag{26a}$$

† It should be noted that, again for convenience, D is defined here as the negative of the function D in the paper of Oppenheim *et al.* (1971).

	Eulerian space	Eulerian time	Lagrangian time
$\frac{t}{t_i}$	1	$\frac{\tau}{\tau_i} = \left(\frac{\phi}{\phi_i}\right)^{-1/\mu}$	$\frac{\tau}{\tau_i} = \left[\frac{Z}{Z_i}\left(\frac{1-F}{1-F_i}\right)^{\gamma-1}\left(\frac{\phi}{\phi_i}\right)^{\alpha}\right]^{(\lambda+2)/(\lambda+2-\alpha)}$
$\frac{r}{r_i}$	$\frac{x}{x_i} = \frac{\phi}{\phi_i}$	1	$\frac{x}{x_i} = \frac{\phi}{\phi_i}\left(\frac{\tau}{\tau_i}\right)^{2/(\lambda+2)}$
$\frac{u}{u_i}$	$\frac{Fx}{F_i x_i}$	$\frac{F\tau_i}{F_i\tau}$	$\frac{Fx\tau_i}{F_i x_i \tau}$
$\frac{\rho}{\rho_i}$	$\left[\frac{Z}{Z_i}\left(\frac{1-F}{1-F_i}\right)^{\nu}\right.$ $\left.\times\left(\frac{x}{x_i}\right)^{(j+1)\nu+2}\right]^{1/(\gamma-1-\nu)}$	$\left[\frac{Z}{Z_i}\left(\frac{1-F}{1-F_i}\right)^{\nu}\left(\frac{\tau_i}{\tau}\right)^{2}\right]^{1/(\gamma-1-\nu)}$	$\left(\frac{1-F_i}{1-F}\right)\left(\frac{x_i}{x}\right)^{j+1}$
$\frac{p}{p_i}$	$\frac{\rho}{\rho_i}\frac{Zx^2}{Z_i x_i^2}$	$\frac{\rho}{\rho_i}\frac{Z\tau_i^2}{Z\tau^2}$	$\left(\frac{\rho}{\rho_i}\right)^{\gamma}$
$\frac{T}{T_i}$	$\frac{Zx^2}{Z_i x_i^2}$	$\frac{Z\tau_i^2}{Z_i\tau^2}$	$\frac{Zx^2\tau_i^2}{Z_i x_i^2 \tau^2}$

TABLE 1. Profiles of gasdynamic parameters

At the same time the remaining two autonomous equations of Oppenheim *et al.* (1971) can be integrated, yielding the so-called adiabatic integral

$$\left(\frac{p}{p_i}\right)\left(\frac{\rho}{\rho_i}\right)^{-\gamma} = \left[\frac{\rho}{\rho_i}\frac{1-F}{1-F_i}\left(\frac{x}{x_i}\right)^{j+1}\right]^{-\nu}, \tag{28}$$

where

$$\nu \equiv \frac{\lambda-(\gamma-1)\omega}{j+1-\omega},$$

which is valid along any line of constant field co-ordinate. Thus, in the above form, (28) applies to the Eulerian space profiles; for the Eulerian time profiles $x = 1$, while for the Lagrangian time profiles the right-hand side is unity.

The $D = 0$ parabola represents the locus of states for which the line of a constant field co-ordinate coincides with a characteristic, that is when the condition $(\partial r/\partial t)_{\phi} = u \pm a$ is satisfied. This fact becomes immediately evident by observing that at ϕ = constant, we have x = constant and τ = constant so that, by virtue of the definitions of (1) and (18), the aforementioned condition yields the $D = 0$ relationship according to (24).

Relations equivalent to (21)–(28) are, of course, well known from the literature (Sedov 1957; Korobeinikov, Mel'nikova & Ryazanov 1961). However, they are presented here in a more concise form, making them especially amenable to the parametric study of their properties with respect to λ and ω that forms the primary objective of this paper. As becomes evident from these equations, the solution is governed by a single differential equation, equation (23), relating the reduced variables F and Z. These variables represent, therefore, the co-ordinates of the phase plane. Once an integral curve on this plane is determined, all the other variables can be evaluated by the quadrature of (21) or (22) and from the algebraic relation given by (28). The resulting expressions for all the

profiles of the gasdynamic parameters of the flow field are presented, with reference to the three fundamental systems of co-ordinates, in table 1.

With respect to the limiting cases, the condition of $\lambda = -2$, corresponding to the exponential front trajectory, does not introduce any anomaly in the governing equations for the Eulerian space profiles. For this case one can thus take simply $\phi = x$ and the transformation to time profiles can be obtained by the use of (19).

In contrast to this the limiting case of $\lambda = \infty$, corresponding to the logarithmic front trajectory, is governed in principle by the time profiles. Hence one now has to take first $\phi = \tau^{-\mu}$; the space profiles are then obtained by using (20). With this provision, the governing equations (21), (22) and (23), are directly applicable to this case while (25), (26) and (28) are, respectively, simplified to

$$Q^*(F, Z) = -\frac{1}{\mu\gamma}[2Z + \gamma(1-F)F], \tag{25b}$$

$$P^*(F, Z) = \frac{1}{\mu}\left[2D(F, Z) - \frac{\gamma-1}{\gamma}\{2Z + \gamma(1-F)F\}\right] \tag{26b}$$

and

$$\rho/\rho_i = (1-F_i)/(1-F). \tag{28a}$$

The latter yields directly the density profile in Eulerian time, which, as pointed out earlier, is the primary system of reference for this case.

4. Properties of the phase plane

Properties of integral curves on the phase plane for self-similar blast waves were a subject of extensive studies in the nineteen fifties. They were summarized in the text of Sedov (1957), where one can find a number of examples of sets of integral curves for some representative values of the velocity parameter μ (denoted by δ by Sedov) and the ambient density parameter ω.

In order to achieve a comprehensive coverage of this field, instead of being concerned with the particular forms of the integral curves which, in view of previous studies, should in any case be considered as generally known, it is more advantageous, now, to examine the loci of their singularities. This is accomplished here by the investigation of the geometrical properties of the loci of extrema in the phase plane, following, in fact, a technique that in recent times has been found particularly useful for the exposition of the salient features of systems governed by nonlinear ordinary differential equations, as demonstrated in the text of Haag (1962).

As is evident from (23), the minima and maxima of the integral curves lie (i) with respect to F: on the $F = 1$ ordinate, or on the $Q = 0$ line, (ii) with respect to Z: on the $Z = 0$ axis, at $Z = \infty$, or on the $P = 0$ line. Hence, besides two fixed singular points at $F = 1$, namely at $Z = 0$ according to (23) and at $Z = \infty$ according to (23*a*), the rest of the singularities involve the conditions $Q = 0$ and/or $P = 0$. Properties on the loci of points satisfying these conditions are therefore investigated in detail. A full list of the physically significant singularities is given in table 2.

Singularity	Condition	Co-ordinates F	Co-ordinates Z	Nomenclature of Sedov
A	$P=0, Q=0, D=0$	$\frac{1}{2}\left[\lambda\frac{2-\gamma}{2j\gamma}+\frac{\omega}{j\gamma}+1\right]$ $-\left[\frac{1}{4}\left(\lambda\frac{2-\gamma}{2i\gamma}+\frac{\omega}{j\gamma}+1\right)^2-\frac{\lambda+\omega}{j\gamma}\right]^{\frac{1}{2}}$	$(1-F_A)^2$	A
G	$P=0, Q=0, D=0$	$\frac{1}{2}\left[\lambda\frac{2-\gamma}{2j\gamma}+\frac{\omega}{j\gamma}+1\right]$ $+\left[\frac{1}{4}\left(\lambda\frac{2-\gamma}{2j\gamma}+\frac{\omega}{j\gamma}+1\right)^2-\frac{\lambda+\omega}{j\gamma}\right]^{\frac{1}{2}}$	$(1-F_G)^2$	—
B	$P=0, Q=0, D\neq 0$	$c=(\lambda+2)/\alpha$	$\frac{(j+1)\gamma(\gamma-1)}{2}$ $\times\frac{(1-F_B)F_B^2}{(j-1)F_B+2-\omega}$	B or ϵ
D	$\hat{Q}=0, \hat{Z}=0$	$b=(\lambda+\omega)/(j+1)\gamma$	∞	D
F	$Q=0, Z=0$	$a=\frac{1}{2}(\lambda+2)$	0	F
O	$F=0, Z=0$	0	0	O
C	$F=1, Z=0$	1	0	C
H	$P=0, F=1$	1	Any value of Z if $\lambda=(\gamma-1)\omega$	—
E	$\hat{P}=0, F=1$	1	∞	ϵ
I	$F=\infty, Z=\infty$	$\pm\infty$	$\pm\infty$	G

TABLE 2. Singularities in the phase plane

Lines Q = constant are given by

$$Z=\frac{(a-F)(1-F)F+Q}{(j+1)(F-b)}. \tag{29}$$

Lines P = constant are expressed by

$$Z=\frac{(1-F)[(\gamma-1)(a-F)F+\alpha(c-F)(1-F)]+P}{(j+1)(\gamma-1)(F-b)+\alpha(c-F)}. \tag{30}$$

For the case of $\lambda=\infty$, the equations for the Q^* = constant and P^* = constant lines are reduced, respectively, to

$$Z=-\tfrac{1}{2}\gamma[(1-F)F+Q^*\mu] \tag{29a}$$

and

$$Z=\tfrac{1}{2}\gamma[2(1-F)\{1-\tfrac{1}{2}(3-\gamma)F\}+P^*\mu]. \tag{30a}$$

According to (26), the $D=0$ line has the property that its intersection with a $Q=0$ line satisfies the condition of $P=0$. It is, therefore, a locus of singularities, i.e. points A and G in table 2, the latter corresponding to the famous Guderley solution for a front-driven implosion into vacuum. The co-ordinates of these

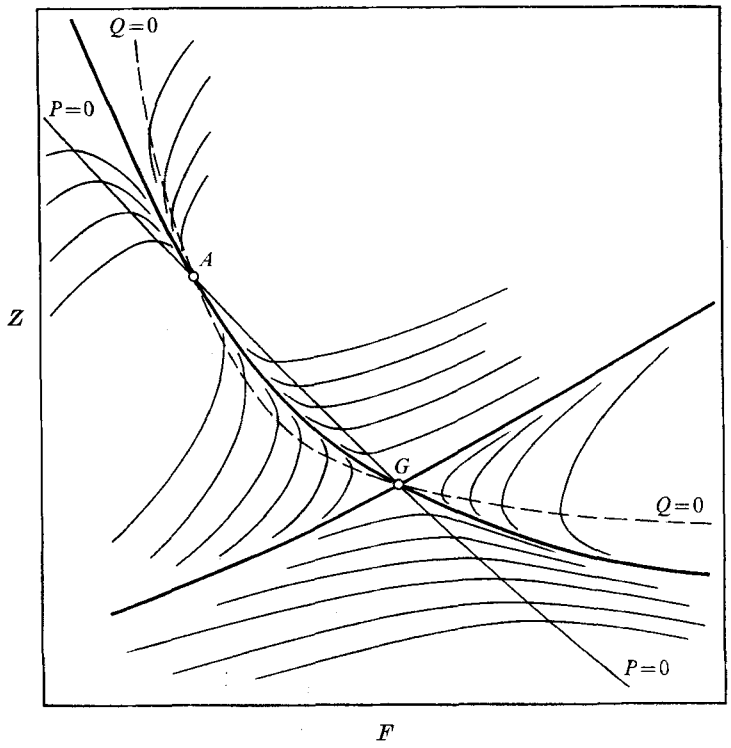

FIGURE 3. Illustration of the relationship between the loci of extrema and singularities in the phase plane. The sketch demonstrates in particular the reason why the A singularity must be a node if the G singularity is a saddle point. The B singularity obtained by another intersection of the same $Q = 0$ and $P = 0$ lines below point G has to be, by the same token, a node.

points given in table 2 have been obtained, in fact, by the solution of (24) and (29) for $Q = 0$. Point G is a saddle point for which the Guderley solution is the axis passing through the origin. As depicted on figure 3, the other axis must pass through, and be shared by, the singularity A. Moreover, as becomes evident from figure 3, this singularity must be then a node since, from purely geometrical considerations, two adjoint intersections of the same loci of extrema can occur only if one is a saddle point and the other is a node (see comments on figure 35 in the text of Haag (1962)).

If $D \neq 0$, then, as is apparent from (26), the condition $Q = 0$ corresponds to $P = 0$, provided that $F = c$. It then follows from the definition (27) that the decay parameter can be expressed in terms of F by the relation $\lambda = \alpha F - 2$. This parameter can therefore be eliminated from (29), yielding

$$B(F, Z) \equiv \{(j-1)F + 2 - \omega\} Z - \tfrac{1}{2}(j+1)\gamma(\gamma-1)(1-F)F^2 = 0. \qquad (31)$$

The singularities whose locus is given here by the condition $B(F, Z) = 0$ were denoted in the text of Sedov (1957) by the letter B.

The remaining singularities of table 2 are situated either on the $F = 0$ axis and $F = 1$ ordinate or on the $Z = 0$ axis and at $Z = \infty$. Their co-ordinates are obtained from the appropriate expressions for the zeros and poles of the $Q = 0$

Condition	Equation	$F(Z=\infty)$	$F(Z=0)$
$Q=0$	$Z=\dfrac{(1-F)(a-F)F}{(j+1)(F-b)}$	$b=\dfrac{\lambda+\omega}{(j+1)\gamma}$	$0, 1$ or $a=\frac{1}{2}(\lambda+2)$
$P=0$	$Z=(1-F)\times\dfrac{(\gamma-1)(a-F)F+\alpha(c-F)(1-F)}{(j+1)(\gamma-1)(F-b)+\alpha(c-F)}$	$1+\dfrac{1}{2\gamma}[\lambda-(\gamma-1)\omega]$	1 or $\left[\dfrac{8+2j(\gamma-1)+(3-\gamma)\lambda}{4\{j(\gamma-1)+2\}}\right] \pm\left[\left(\dfrac{8+2j(\gamma-1)+(3-\gamma)\lambda}{4\{j(\gamma-1)+2\}}\right)^2-\dfrac{\lambda+2}{j(\gamma-1)+2}\right]^{\frac{1}{2}}$
$D=0$	$Z=(1-F)^2$	$\mp\infty$	1
$B=0$	$Z=\dfrac{(j+1)\gamma(\gamma-1)}{2}\times\dfrac{(1-F)F^2}{(j-1)F+2-\omega}$	$\dfrac{\lambda+2}{\alpha}=\dfrac{\omega-2}{j-1}$	0 or 1

TABLE 3. Properties of the lines $P=0$, $Q=0$, $D=0$ and $B=0$

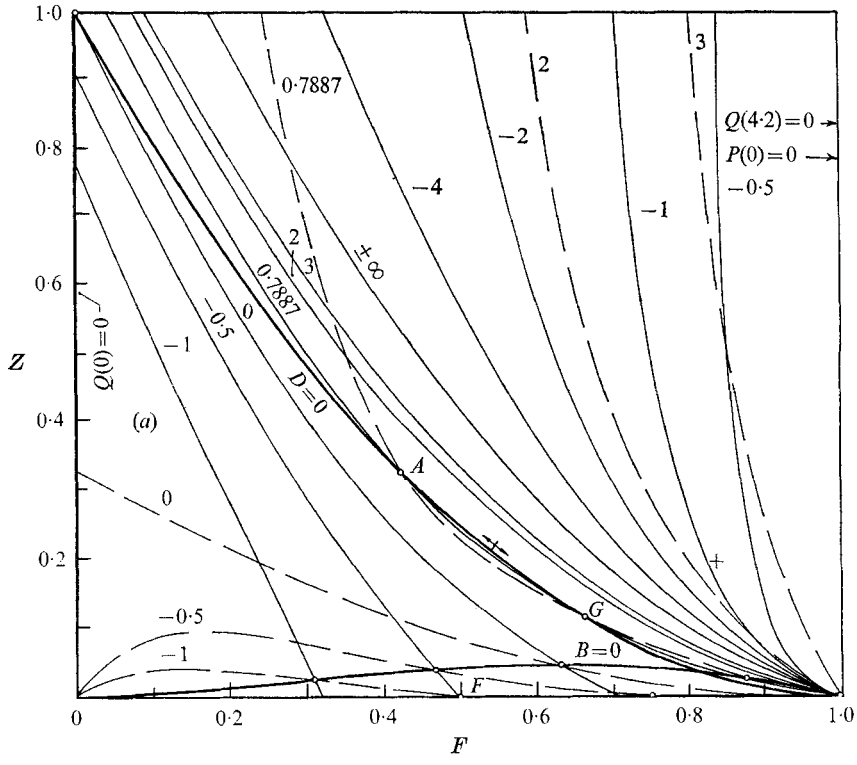

FIGURE 4. Loci of extrema and of singularities in the phase plane ($j=2, \gamma=1{\cdot}4$). ——, $P=0$ lines; — — —, $Q=0$ lines; ○, singular points obtained by intersections of the appropriate loci of extrema; +, strong-shock boundary condition. (*a*) Uniform-density atmosphere, curves labelled with values of the decay parameter λ. (*b*) Constant front velocity waves, curves labelled with values of the atmospheric density parameter ω. (*c*) Constant-energy waves, curves labelled with values of ω.

For figures 4(*b*) and (*c*) see facing page.

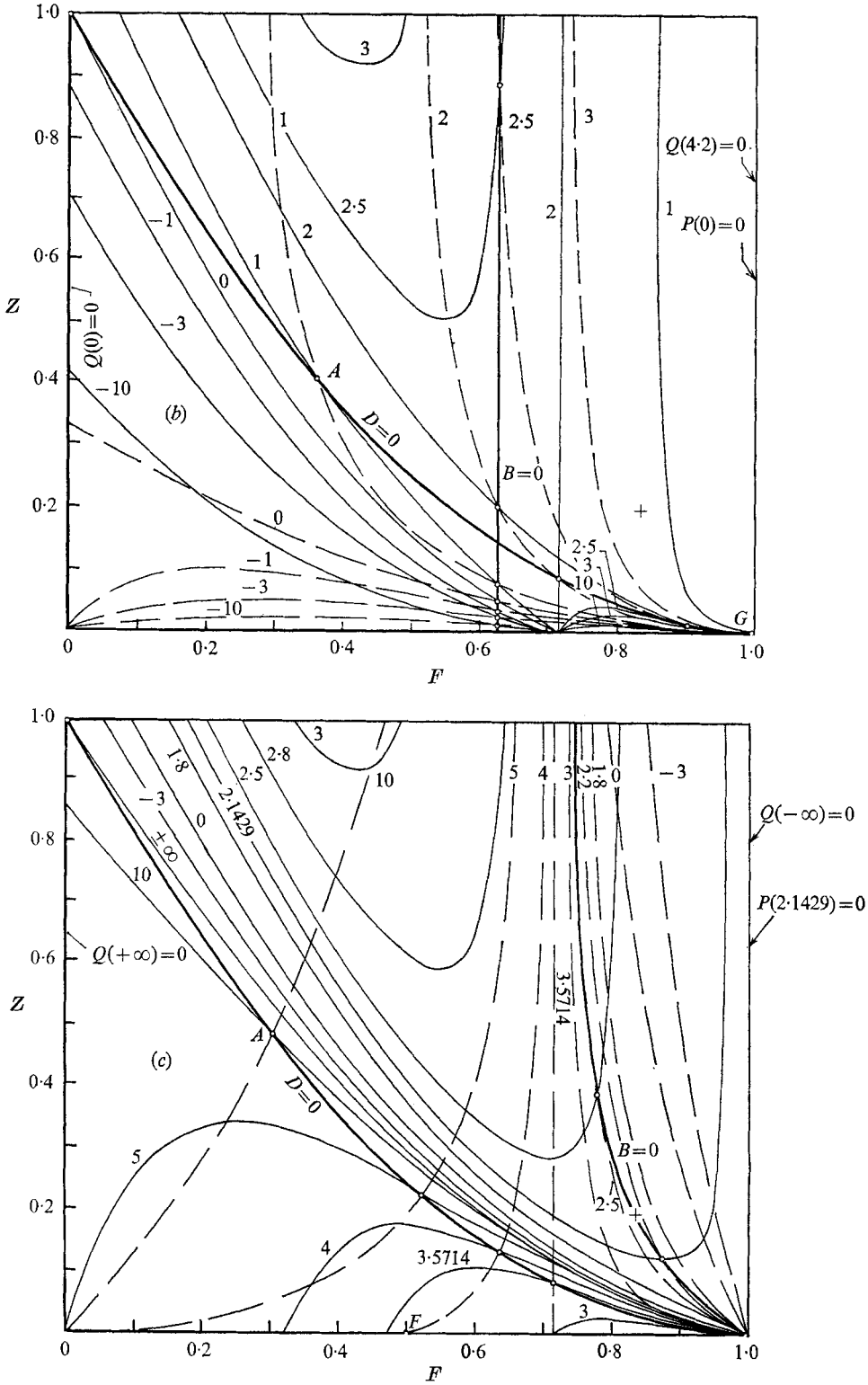

FIGURES 4(*b*) and (*c*).

and $P = 0$ lines, which, one should note, are poles and zeros for the $\hat{Q} = 0$ and $\hat{P} = 0$ lines. These are listed in table 3.

Loci of the $Q = 0$ and $P = 0$ lines are presented in figures 4(*a*), (*b*) and (*c*), corresponding, respectively, to the following three cases: (i) waves of variable front velocity in an atmosphere of uniform density, i.e. $\lambda \neq 0$, $\omega = 0$, (ii) waves of constant front velocity in an atmosphere of variable density, i.e. $\lambda = 0$, $\omega \neq 0$, (iii) waves of constant energy in an atmosphere of variable density, i.e. $\lambda = j + 1 - \omega$ (the relationship which, as is immediately evident from equation (16) in the paper of Oppenheim *et al.* (1971), reduces the energy equation, under the aforementioned self-similarity restrictions, to a constant-energy condition). All the diagrams have been computed for $\gamma = 1{\cdot}4$. The $Q = 0$ lines are represented by broken lines, while the $P = 0$ lines are continuous. In figure 4(*a*) each line is labelled by the value of λ, while in figures 4(*b*) and (*c*) curves are labelled by the value of ω. The loci of singularities associated with the intersections of the $Q = 0$ lines with the $P = 0$ lines, namely the $D = 0$ parabola and the $B = 0$ curve, are represented in all the diagrams by heavy lines. Typical singularities corresponding to the same fixed values of the parameter λ or ω are indicated by circles. The cross denotes the strong-shock boundary condition (see figure 6). The A and G singularities marked in figure 4(*a*) correspond to the λ of the Guderley solution, that is, the integral curve passing from the strong shock boundary condition to the origin. The value of λ_G given in figure 4(*a*) is that obtained by Lee (1967); the co-ordinates of points A and G are then given by the appropriate expressions in table 2.

It should be observed that the functions $D(F, Z)$, $Q(F, Z)$ and $P(F, Z)$ have been defined here so that they are positive for $Z > Z(D = 0)$, $Z > Z(Q = 0)$ and $Z > Z(P = 0)$. Taking this into account, one can deduce from (21) and (22) the direction corresponding to an increasing value of the self-similar field co-ordinate ϕ for any integral curve, as it has been done, for instance, in figure 7, where such directions have been indicated by arrows. Thus integral curves with arrows pointing towards the point corresponding to conditions at the front represent explosions and those with arrows pointing in the opposite direction represent implosions.

Of particular interest are the cases when the $P = 0$ or $Q = 0$ lines are vertical. Since their equations are then satisfied for any value of Z, they correspond to the conditions of coincidence between the zeros and the poles of table 3. The expressions for the parameters λ and ω and the values of the co-ordinate F corresponding to these cases are given in table 4. The corresponding lines are easily identifiable on figures 4(*a*), (*b*) and (*c*). If such a line for $P = 0$ coincides with the ordinate $F = 1$, it becomes a locus of singularities. This is indeed the case for the conditions of the first, third and seventh column of table 4. The singularity situated on this line is then a saddle point (see figure 5) and the $F = 1$ ordinate is one of its axes. The other axis is determined by the appropriate integral curve, that is, one for $\lambda = 0$ in figure 4(*a*), for $\omega = 0$ in figure 4(*b*), and for $\omega = (j + 1)/\gamma$ in figure 4(*c*).

As is apparent from table 2, the positions of the first five singularities depend on the values of the parameters λ and ω. The phase plane co-ordinate F for these

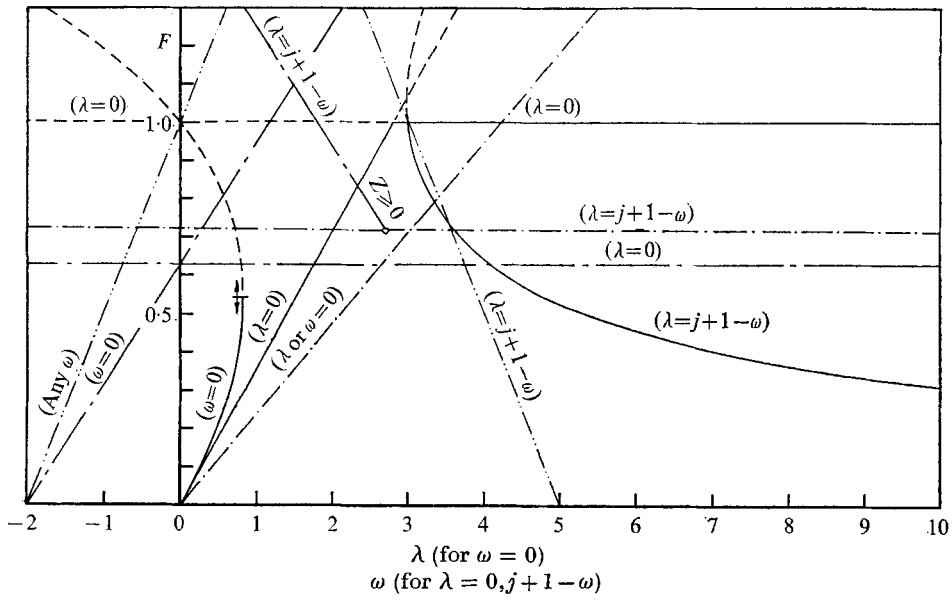

FIGURE 5. Phase plane co-ordinate F for non-fixed singularities as a function of the parameters λ and ω. ———, singularity A; — — —, G; — — —, B; —·—, D; —··—, F.

	Figure 4(*a*)		Figure 4(*b*)			Figure 4(*c*)		
ω	0	0	0	$(j+1)\gamma$	2	$-\infty$	$(j+1)/\gamma$	$j+3-2/\gamma$
λ	0	$(j+1)\gamma$	0	0	0	$j+1-\omega$	$j+1-\omega$	$j+1-\omega$
$F(Q=0)$	0	1	0	1	—	0	—	$1/\gamma$
$F(P=0)$	1	—	1	—	$1/\gamma$	—	1	—

TABLE 4. Cases for which the loci of extrema are satisfied for any value of Z

singularities is shown plotted as a function of λ and ω in figure 5 for the case of spherical waves in a perfect gas with $\gamma = 1{\cdot}4$.

5. Boundary conditions

In this paper we restrict our attention to the physically most prevalent situations which, with reference to boundary conditions, is tantamount to limiting ourselves to the case where the atmosphere into which the wave propagates is at rest.

For a gas with γ = constant the phase plane co-ordinates of the points representing the boundary conditions can be expressed in terms of the following relations (see Oppenheim *et al.* 1971):

$$F_n = \frac{2}{\gamma+1}\frac{P-P_G}{P+\beta} \tag{32}$$

and

$$Z_n = \frac{2\gamma}{\gamma+1}[(P_G+\beta)+\beta(P-P_G)]\frac{P-P_G}{P+\beta}\frac{P}{P-1}, \tag{33}$$

where $\beta \equiv (\gamma-1)/(\gamma+1)$, $P \equiv p_n/p_a$, p being the pressure, subscript n denoting conditions immediately behind the shock front and subscript a referring to the state of the ambient atmosphere.

$$P_G = (\gamma-1)\left\{\frac{1}{\gamma_a-1}+\frac{\gamma_a q}{a_a^2}\right\} = (\gamma-1)\left\{\frac{\gamma}{\gamma-1}\nu_F-1\right\} \tag{34}$$

is the pressure ratio attained by the process of the deposition in the gas of energy q per unit mass at constant volume and ν_F is the specific volume ratio for the corresponding process at constant pressure.

By eliminating P from (32) and (33) one obtains the following equation for the Hugoniot curve in the phase plane:

$$Z_n = \frac{\gamma-1}{2}\frac{F_n+[2/(\gamma-1)]P_G}{F_n+(1/\gamma)(P_G-1)}(1-F_n)F_n, \tag{35}$$

which for $P_G = 1$ reduces to the Rankine–Hugoniot relation

$$Z_n = \tfrac{1}{2}(\gamma-1)(F_n+2/(\gamma-1))(1-F_n). \tag{35a}$$

For $P_G = \infty$, corresponding to the case of cold atmosphere or zero-counter-pressure, it becomes simply

$$Z_n = \gamma(1-F_n)F_n. \tag{35b}$$

At the same time the equation of the Rayleigh line,

$$\gamma M_n^2 = (P-1)/(1-\nu), \tag{36}$$

where M_n is the front Mach number and $\nu \equiv \rho_a/\rho_n$, can be transformed by using the definitions of (16) and noting that, on the basis of the continuity equation, $F_n = 1-\nu$ into

$$Z_n = (Z_a+\gamma F_n)(1-F_n), \tag{36a}$$

where

$$Z_a = 1/M_n^2 \equiv y. \tag{37}$$

It is of interest to note that for the case of $Z_a = y = 0$ the Rayleigh line in the phase plane coincides with the Hugoniot curve for $P_G = \infty$.

The intersections between the Rayleigh lines and the Hugoniot curves are given by the expression

$$F_n = \frac{1-y}{1+\gamma} \pm \left[\left(\frac{1-y}{1+\gamma}\right)^2 - \frac{2y}{\gamma(\gamma+1)}(P_G-1)\right]^{\frac{1}{2}}, \tag{38}$$

which, for the intersections with the Rankine–Hugoniot curve, is reduced to

$$F_n = 2(1-y)/(1+\gamma). \tag{38a}$$

Plots of the Hugoniot curves and the Rayleigh lines are presented for the case of $\gamma = 1{\cdot}4$ in figure 6. The $D = 0$ line, representing in this case the locus of the Chapman–Jouguet conditions, is shown there by a broken line.

All the integral curves representing a blast wave whose front is a discontinuity that propagates into an atmosphere at rest must pass through the region bounded by the two extreme Hugoniot curves, namely those corresponding to $P_G = 1$ (Rankine–Hugoniot) on one side and $P_G = \infty$ on the other. In this connexion it

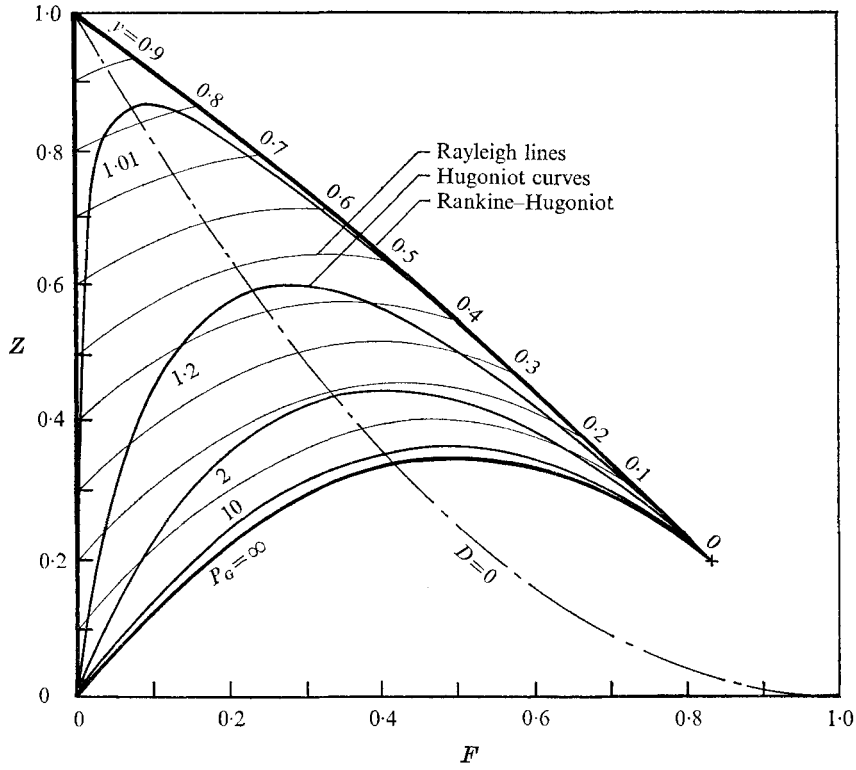

FIGURE 6. Loci of states immediately behind fronts propagating into a medium at rest ($\gamma = 1{\cdot}4$). The physically realizable cases for combustion systems are restricted to the area bounded by the Rankine–Hugoniot curve, the $P_G = \infty$ line and the $D = 0$ parabola.

is of interest to note how rapidly an increase in the value of P_G causes the Hugoniot curves to approach the case of $P_G = \infty$, the curve corresponding to $P_G = 10$ being practically coincident with this limit.

The $D = 0$ parabola represents the locus of the Chapman–Jouguet conditions and it separates the regions of strong detonations on the right from weak detonations on the left. Since in the course of chemical explosions weak detonations may not be sustained, the most physically relevant extent of boundary conditions is in this case confined to the small region between this line and the Rankine–Hugoniot curve. Moreover, in order to satisfy the self-similarity requirements, this region can be considered as a locus of boundary conditions only for constant-velocity blast waves (i.e. just for $\lambda = 0$) in the case of uniform velocity of sound in the ambient atmosphere, that is, if $\omega = 0$ or, if $\omega \neq 0$, when $p_a \propto \rho_a$. Otherwise only the $P_G = \infty$ line can be admitted as the locus of boundary conditions at the fronts of self-similar blast waves.

6. Wave structure

As an illustration of the structure of self-similar waves, a complete set of solutions is presented here for the shock-bounded case corresponding to $\omega = 0$. The only admissible boundary condition is then that associated with $y = 0$ or

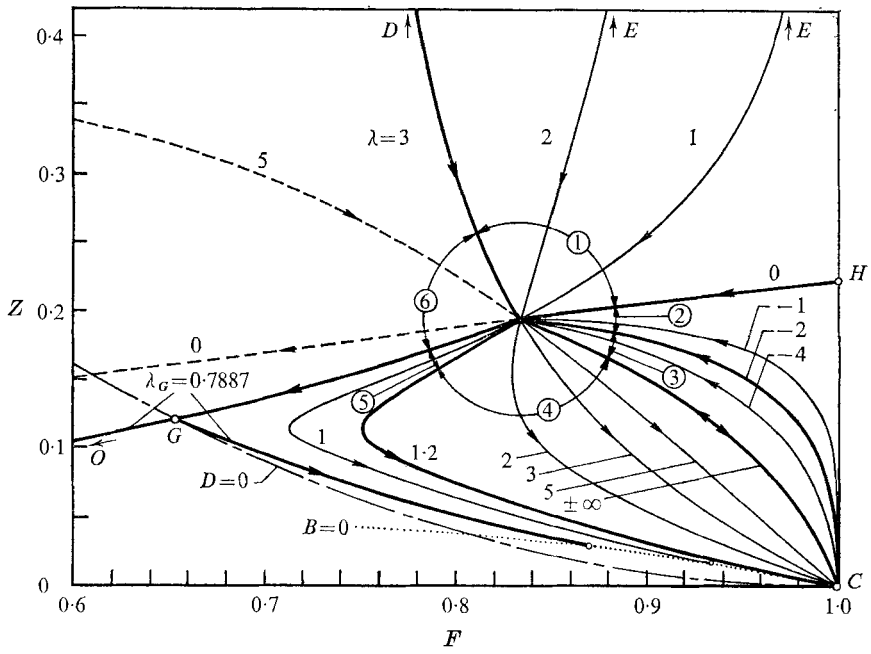

FIGURE 7. Integral curves in the phase plane for waves bounded by a strong-shock front moving into a uniform-density atmosphere at rest ($j = 2, \gamma = 1{\cdot}4$). Arrows denote the direction of increasing x; integral curves for which they point towards the point representing the boundary condition correspond to explosions, those for which they point in the opposite direction correspond to implosions. Front trajectories for the solutions presented here are depicted on figure 2.

$P_G = \infty$. According to (38a) and (35b), all the integral curves have, therefore, to pass through the point

$$F_n = \frac{2}{\gamma+1}, \quad Z_n = \frac{2\gamma(\gamma-1)}{(\gamma+1)^2}. \tag{39}$$

A set of integral curves satisfying this requirement is shown for the case of $j = 2$ and $\gamma = 1{\cdot}4$ in figure 7 and the corresponding velocity, density, pressure and temperature (or sound speed) profiles in the Eulerian-space co-ordinates are given in figures 8, 9, 10 and 11 respectively. The best known of the solutions shown on these graphs is that corresponding to the blast wave of constant energy of value one for

$$\lambda = j+1-\omega, \tag{40}$$

when, as pointed out earlier, the differential energy equation can be integrated immediately, yielding the constant-energy condition.

By using (40) and noting that the expression for the locus of singularities B, equation (31), corresponds to $\lambda = \alpha F - 2$, the $B = 0$ line can be expressed in terms of the relation

$$Z = \frac{\gamma-1}{2}\frac{(1-F)F^2}{F-1/\gamma}. \tag{41}$$

This equation satisfied the strong-shock boundary condition (39) and is also a particular solution of the governing differential equation (23). Thus the locus of

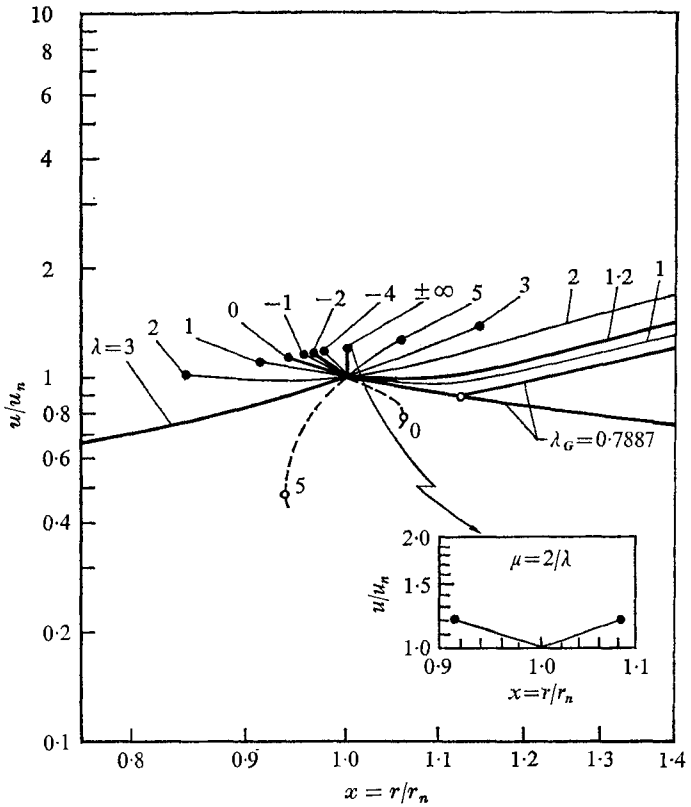

FIGURE 8. Particle velocity profiles for waves bounded by a strong-shock front propagating into a uniform-density atmosphere at rest ($j = 2, \gamma = 1{\cdot}4$). ●, piston; ○, $D = 0$. Profiles for the limiting case of waves with logarithmic front trajectories corresponding to $\lambda = \pm\infty$ are shown in the insert.

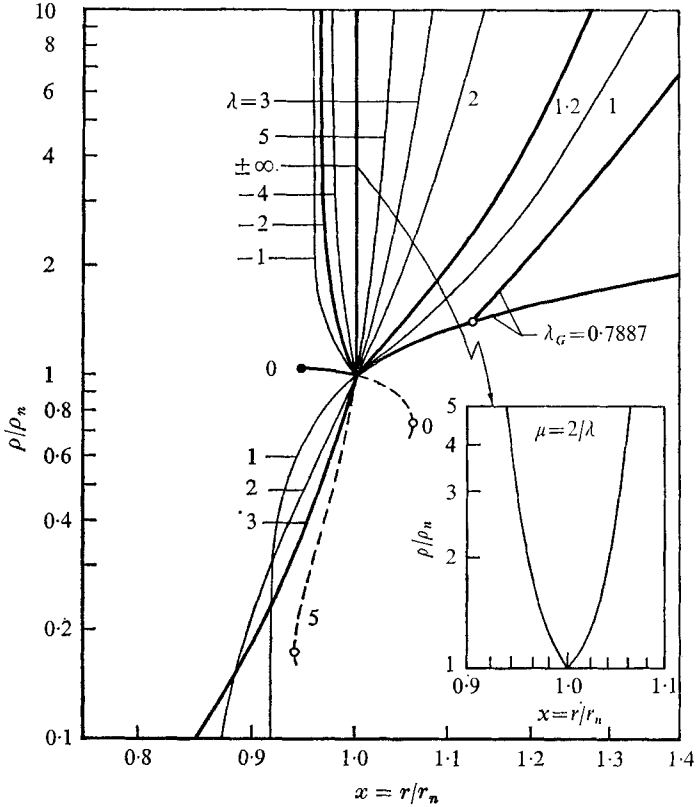

FIGURE 9. Density profiles for waves bounded by a strong-shock front propagating into a uniform-density atmosphere at rest ($j = 2, \gamma = 1{\cdot}4$). ●, piston; ○, $D = 0$. Profiles for the limiting case of waves with logarithmic front trajectories corresponding to $\lambda = \pm\infty$ are shown in the insert.

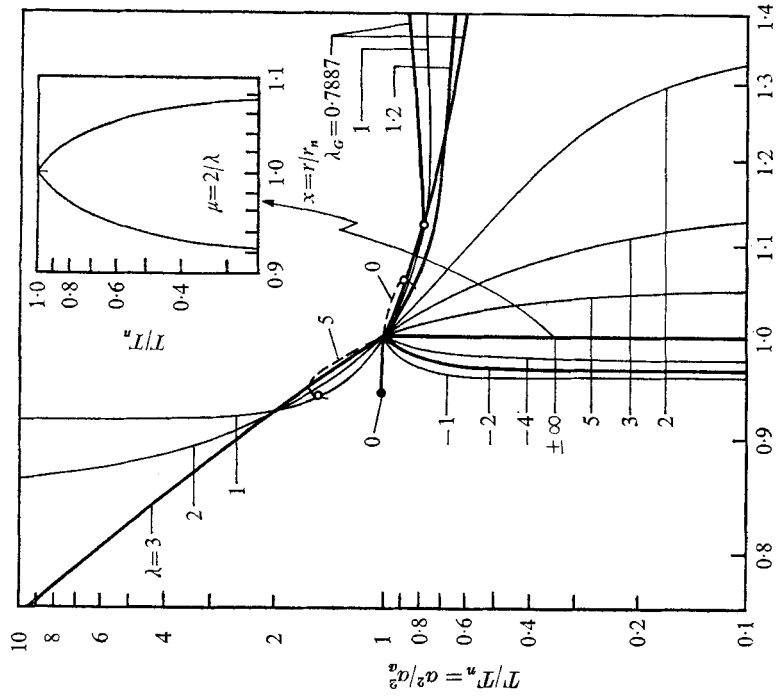

FIGURE 11. Temperature or velocity of sound profiles for waves bounded by a strong-shock front propagating into a uniform-density atmosphere at rest ($j = 2$; $\gamma = 1{\cdot}4$). ●, piston, ○, $D = 0$. Profiles for the limiting case of waves with logarithmic front trajectories corresponding to $\lambda = \pm\infty$ are shown in the insert.

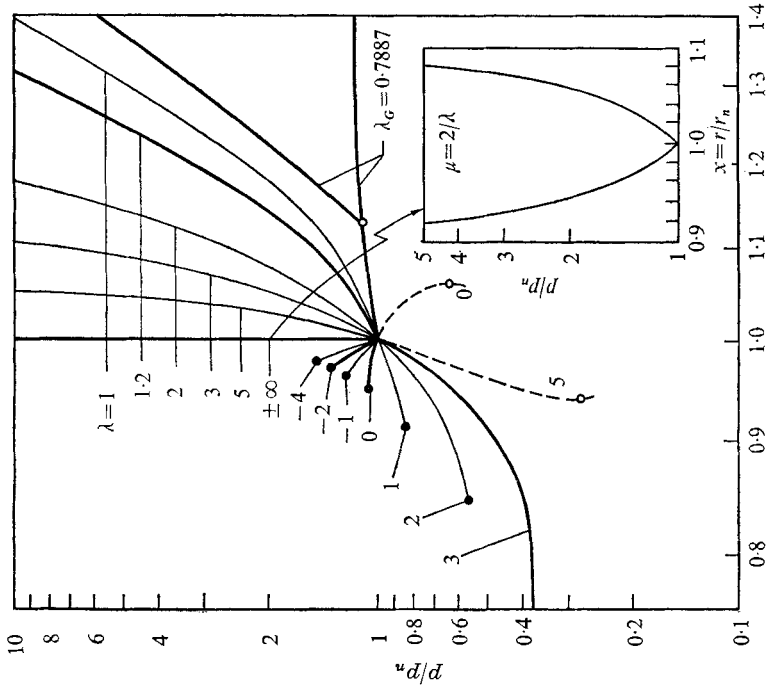

FIGURE 10. Pressure profiles for waves bounded by a strong-shock front propagating into a uniform-density atmosphere at rest ($j = 2$; $\gamma = 1{\cdot}4$). ●, piston; ○, $D = 0$. Profiles for the limiting case of waves with logarithmic front trajectories corresponding to $\lambda = \pm\infty$ are shown in the insert.

singularities B in figure 4 (c) is at the same time an integral curve and the solution of the constant-energy self-similar blast wave in figure 7: a remarkable coincidence! As a consequence of this, the structure of the blast wave can be expressed in terms of an algebraic solution. Thus, taking into account (41), (21) becomes

$$\frac{d\ln\phi}{d\ln F} = \frac{1}{\alpha}\frac{\gamma(\gamma-1)F^2 - 2(\gamma F-1)(1-F)}{(\gamma F-1)(c-F)}, \tag{42}$$

yielding

$$\phi = \left(\frac{F}{F_n}\right)^{-2/(\lambda+2)}\left(\frac{\gamma F-1}{\gamma F_n-1}\right)^{d_1}\left(\frac{c-F}{c-F_n}\right)^{d_2}, \tag{43}$$

where

$$d_1 \equiv \frac{\gamma-1}{\alpha(\gamma c-1)}, \quad d_2 \equiv -\frac{2+(\gamma+1)(\gamma c-2)c}{\alpha c(\gamma c-1)}.$$

Equations (41) and (43) describe completely the structure of the wave in terms of the co-ordinate F and on the basis of these equations, profiles of all the gasdynamic parameters can be obtained from the expressions given in table 1.

Under the conditions of figure 7, the integral curve representing the constant-energy blast wave corresponds to $\lambda = 3$. The curves corresponding to $0 < \lambda < 3$, i.e. those in sector (1) of figure 7, pass through singularity E ($F = 1$, $Z = \infty$). They represent, therefore, blast waves driven by a piston at infinite temperature. The curve for the case $\lambda = 0$, corresponding to a piston driven wave of constant front velocity passes through singularity H, a saddle point, and it thus separates this set of solutions from that converging upon the singularity C ($F = 1$, $Z = 0$). For $-\infty < \lambda < 0$, in sectors (2) and (3) of figure 7, the integral curves represent explosions driven by a piston at zero velocity of sound (or temperature). The two sectors are separated by the integral curve for $\lambda = -2$ which, as was discussed above, can be considered as a limiting case of an exponential front trajectory. The curve corresponding to $\lambda = \infty$ can also be considered to represent the limiting case of a logarithmic front trajectory. Solutions for this case can be obtained by using (25b), (26b) and (28a).

Integral curves on the left of the $\lambda = \infty$ line in sector (4) represent implosions driven by a piston at infinity, while the zero velocity of sound condition is still retained. The curve for $\lambda = \alpha - 2 = (j+1)(\gamma-1)$, i.e. $\lambda = 1{\cdot}2$ in figure 7, corresponds to the case where the condition $B(F, Z) = 0$ of (31) is satisfied at $F = 1$. It terminates, therefore, at a singular point corresponding to a finite velocity of sound (or temperature). For $\lambda_G < \lambda \leqslant (j+1)(\gamma-1)$, in sector (5), the integral curves terminate at the B singularity, and $Z > 0$ and $F < 1$. This corresponds to conditions at infinity, where both the temperature and the velocity are infinite, but the particle path does not coincide with the trajectory of a constant field co-ordinate, i.e. the waves are not piston driven.

Sector (5) in figure 7 is bounded by the curvilinear axis of the Guderley singularity: a saddle point. By virtue of the fact that at this point the two pairs of functions $Q(F, Z)$ and $D(F, Z)$ in (21), and $P(F, Z)$ and $D(F, Z)$ in (22) change signs, the integral curve passing through this singularity is associated with monotonic variation of the field co-ordinate across it. This curve represents, therefore, a physically meaningful solution leading to the singular point O ($F = 0$, $Z = 0$), where, both the particle velocity and the velocity of

sound can have finite values at infinity. In sector (6), between the lines corresponding to the constant-energy explosion and the Guderley implosion, integral curves have no physical meaning since, as is demonstrated by the broken lines in figures 8–11, as a consequence of the intersection with the $D = 0$ line the gasdynamic parameters of the flow field become double-valued functions of the field co-ordinate.

The front trajectories for all the solutions represented in figure 7 have been depicted in figure 2, while all the information on the structure is given by the profiles of the gasdynamic parameters presented in figures 8–11, where, incidentally, the explosions are clearly differentiated from implosions by the fact that for the former $x < 1$ while for the latter $x > 1$.

Inserts in figures 8–11 give solutions for the limiting case corresponding to $\lambda = \pm\infty$, that is for blast waves with logarithmic trajectories. They were obtained by the use of the transformation prescribed by (20). As pointed out before, the limiting case corresponding to $\lambda = -2$, associated with blast waves with exponential trajectories, does not involve any anomaly in the Eulerian space system of reference. Thus the solutions of figures 7–11 represent a complete set of all possible cases that can occur for self-similar blast waves bounded by shock fronts in an atmosphere of uniform density, including the limiting cases of logarithmic and exponential trajectories.

A similarly complete coverage can, of course, be obtained for any other point on the $P_G = \infty$ line. A representative solution for one of such cases has been obtained recently by Champetier, Couairon & Vendenboomgaerde (1968) and by Wilson & Turcotte (1970) with reference to blast waves driven by laser irradiation. Assuming that in this case the wave receives energy at a constant power level, p, they postulated on the basis of a dimensional argument that the front trajectory is then prescribed by a power law of the type given in (8) with $\mu_p = \frac{3}{5}$. From (7) it follows then that $\lambda_p = \frac{4}{3}$. The corresponding integral curve, obtained by using (23a), is shown in figure 12. Such solutions terminate with $\lambda = \frac{7}{9}$ at the point of intersection between $P_G = \infty$ curve and the $D = 0$ line (the boundary condition of the strong Chapman–Jouguet detonation), which for this value of λ represents also the position of singularity A. Under such circumstances one can have a degenerate solution.

In general, degenerate solutions can occur when, as it has been pointed out by Sedov (1957), the point specifying the boundary condition coincides with a singularity. Besides the integral curve, this point can be considered to represent also a solution, so that the wave structure may correspond then to the condition $F = F_n =$ constant and $Z = Z_n =$ constant. In table 1 all the terms involving F and Z are, under such circumstances, reduced to unity and the profiles of the gasdynamic parameters then become simple powers of the field co-ordinate. In figure 12 the loci of all the points that can be considered as degenerate solutions are represented by heavy line segments with limits delineated by the appropriate $B = 0$ lines.

In the case of $\lambda = 0$, degnerate solutions can be obtained either if the boundary condition coincides with singularity A on the $D = 0$ curve or with singularity B on the $B = 0$ line at $F = 2/\alpha$ (or $F = 0{\cdot}625$ for $j = 2$ and $\gamma = 1{\cdot}4$). The range

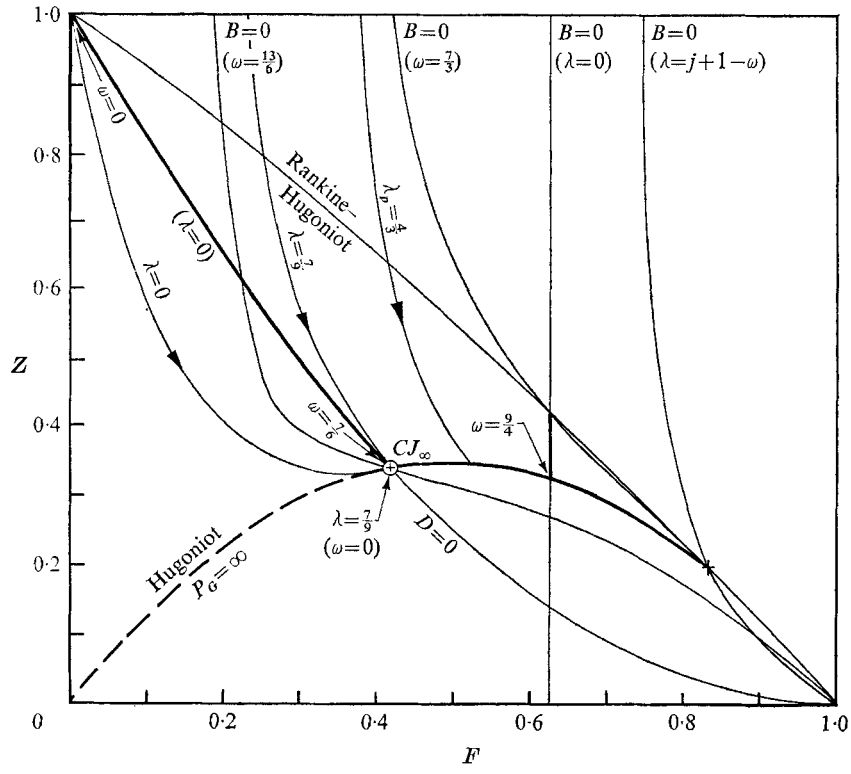

FIGURE 12. Integral curves representing particular solutions of waves bounded by detonation fronts and loci of degenerate solutions. Also shown are the $B = 0$ lines passing through the points representing the extreme cases of the degenerate solutions. Arrows denote the direction of increasing x.

within which singularity A can represent a degenerate solution is bounded by the weak discontinuity at $F = 0$, $Z = 1$ on one side and the CJ_∞ point on the other, corresponding to $\omega = 0$ and $\omega = j\gamma/(\gamma+1)$, respectively (or $0 \leqslant \omega \leqslant \frac{7}{6}$ for $j = 2$ and $\gamma = 1{\cdot}4$). The segment of the $B = 0$ line that can serve the same purpose is bounded by the $P_G = \infty$ parabola and the Rankine–Hugoniot curve, corresponding, respectively, to $\omega = 1+2j/\alpha$ and $\omega = 2+2(j-\gamma)/(\alpha+\gamma-1)$ (or $\frac{9}{4} \leqslant \omega \leqslant \frac{7}{3}$ for $j = 2$ and $\gamma = 1{\cdot}4$).

In the case of $\lambda \neq 0$ while $\omega =$ constant, degenerate solutions occur when the B singularity coincides with a point on the $P_G = \infty$ line, or when singularity A is situated at the CJ_∞ point. The range within which singularity B has in this case to be contained is bounded by the CJ_∞ point, for which now

$$\omega = 2+(2j-\alpha)/2(\gamma+1) \quad \text{and} \quad \lambda = \alpha/(\gamma+1)-2$$

(or $\omega = 1\frac{3}{6}$ and $\lambda = -\frac{2}{3}$ for $j = 2$ and $\gamma = 1{\cdot}4$), and the strong-shock boundary condition when

$$\omega = 2+(2j-\alpha)/(\gamma+1) \quad \text{and} \quad \lambda = 2\alpha/(\gamma+1)-2$$

(or $\omega = \frac{7}{3}$ and $\lambda = \frac{2}{3}$ for $j = 2$ and $\gamma = 1{\cdot}4$). The appropriate values for λ have been deduced from the condition for the B singularity: $F = (\lambda+2)/\alpha$. The weak

detonation branch of the $P_G = \infty$ line, that is, the segment of this line below the CJ_∞ point, is ruled out on physical grounds. Since at the CJ_∞ condition $y = 0$, the point representing this state can coincide with an A singularity, when, unlike the previously discussed degenerate cases involving this singularity, $\lambda \neq 0$. Thus, from the expression for the position of the A singularity given in table 2 and the co-ordinate of the CJ_∞ point ($F = 1/(\gamma+1)$, $Z = [\gamma/(\gamma+1)]^2$), one finds that this can happen if $\omega = 0$ and $\lambda = \frac{2}{3}j\gamma/(\gamma+1)$, which for $j = 2$ and $\gamma = 1{\cdot}4$ yields the aforementioned value of $\lambda = \frac{7}{9}$, as noted on figure 12.

Besides the degenerate solution represented by the CJ_∞ point, there also exists a family of integral curves corresponding to $\lambda = \frac{7}{9}$ that pass through this point. Although a full discussion of the properties of such 'variable-velocity Chapman–Jouguet detonations' has been considered to be outside the scope of the present paper, the solution for the most important one, namely that of a front-driven wave corresponding to the integral curve passing through singularity D, is shown in figure 12. This figure also includes the integral curve for $\lambda = 0$ passing through the CJ_∞ point. It represents the structure of a blast wave bounded by a strong Chapman–Jouguet front moving at a constant velocity. The end state of $F = 0$ and $Z = 1$ is attained at a finite value of x, so that this blast wave has a core at rest. Under the conditions of figure 14 the front of the core is at a radius $r_c = 0{\cdot}4874r_n$, while the pressure and density in the core are, respectively, $p_c = 0{\cdot}2760p_{CJ}$ and $\rho_c = 0{\cdot}3987\rho_{CJ}$.

Integral curves passing through the CJ_∞ point for values of λ in the interval $0 < \lambda < \frac{7}{9}$ have no physical meaning since they cross the $D = 0$ line. On the other hand, the integral curve for $\lambda = 0$ shown in figure 12 bounds a family of similar curves passing through any point of the $D = 0$ line between the CJ_∞ point and the weak discontinuity at $Z = 1$. They all pass through the point $F = 0$, $Z = 1$ since, for $\lambda = 0$, it is the position of singularity A. Points on the $D = 0$ line below the CJ_∞ point are outside the regime of boundary conditions for waves propagating into an atmosphere at rest and integral curves passing through them are considered to be outside the scope of the present paper.

7. Summary and conclusions

A comprehensive treatment of self-similar blast waves has been given here with respect to two parameters, one describing the trajectory of the front in the time–space domain and the other the variation in the density of the medium into which the wave propagates. Three fundamental cases have been covered: one corresponding to uniform-density atmosphere, the second to constant front velocity and the third to constant wave energy when the two parameters are interrelated algebraically. This comprehensive character has been attained primarily as a result of a more concise formulation of the theory than those of the authors of the many publications available on this subject. Thus, most of the known solutions have been correlated and their properties generalized, covering all the possible values of the aforementioned parameters that are of physical significance for waves propagating into a medium at rest with respect to their centres of symmetry.

Moreover, the analytical facility afforded by the simpler formulation permitted the determination of some particular properties which have not been recorded in the literature. The most important in this respect was a thorough investigation of the phase plane of the solutions defined in terms of the reduced co-ordinates $F = (t/r\mu)\,u$ and $Z = [(t/r\mu)\,a]^2$ defined above. This was accomplished by tracing the loci of extrema of the integral curves in this plane and of their intersections fixing the loci of singularities. In this way the reasons for the occurrence of the singularities and the dependence of their position on the values of the two parameters could be fully explored. Hence, besides covering all the known cases of singular points, the existence of a number of singularities not yet singled out in the literature has been established.

On this basis all the salient features of the wave structure have been determined, covering the full range of physically meaningful solutions pertaining to shock fronts propagating into an atmosphere of uniform density, including the limiting cases of exponential and logarithmic front trajectories. Particular solutions in the phase plane for waves bounded by detonation fronts have also been obtained and all the degenerate solutions for which the integral curves on the phase plane are reduced to single points have been pinpointed.

This work was supported by the United States Air Force through the Air Force Office of Scientific Research under Grant AFOSR 129-67, by the National Aeronautics and Space Administration under Grant NsG-702/05-003-050 and by the National Science Foundation under Grant NSF GK-2156.

REFERENCES

Bruslinskii, K. V. & Kazdan, Ja. M. 1963 Self-similar solutions of certain problems in gasdynamics. *Uspehi Mat. Nauk*, **18**, 3–32.

Butler, D. S. 1954 Converging spherical and cylindrical shocks. *British Ministry of Supply, Armament Research Establishment Rep.* no. 54.

Champetier, J. L., Couairon, M. & Vendenboomgaerde, Y. 1968 On blast waves generated by lasers. *C.R. Acad. Sci. Paris*, **267** (B 74), 1133–1136.

Courant, R. & Friedrichs, K. O. 1948 *Supersonic Flow and Shock Waves*, p. 464. Wiley.

Grigorian, S. S. 1958*a* Cauchy's problem and the problem of a piston for one-dimensional non-steady motions of a gas. *J. Appl. Math. Mech.* **22**, 187–197.

Grigorian, S. S. 1958*b* Limiting self-similar one-dimensional non-steady motion of a gas (Cauchy's problem and the piston problem). *J. Appl. Math. Mech.* **22**, 301–310.

Grodzovskii, G. L. 1956 Self-similar motion of a gas with a strong peripheral explosion. *Dokl. Akad. Nauk, S.S.S.R.* **111**, 969–971.

Guderley, G. 1942 Powerful spherical and cylindrical compression shocks in the neighbourhood of the centre of the sphere and of the cylinder axis. *Luftfahrtforschung*, **19**, 302–312.

Haag, J. 1962 *Oscillatory Motions* (trans. R. M. Rosenberg), p. 201. Belmont, California: Wadsworth Publishing Co.

Hayes, W. D. 1968 Self-similar strong shocks in an exponential atmosphere. *J. Fluid Mech.* **32**, 305–315.

Kochina, N. N. & Mel'nikova, N. S. 1960 On the motion of a piston in an ideal gas. *J. Appl. Math. Mech.* **24**, 307–315.

KOROBEINIKOV, V. P., MEL'NIKOVA, N. S. & RYAZANOV, YE. V. 1961 *The Theory of Point Explosion.* Moscow: Fizmatgiz. (Trans. 1962 U.S. Dept. of Commerce, JPRS: 14, 334, CSO: 6961-N, Washington.)

KRASHENINNIKOVA, N. L. 1955 On unsteady motion of gas forced out by a piston. *Izv. Akad. Nauk S.S.S.R., otd. Tekh. Nauk*, **8**, 22–36.

LEE, B. H. K. 1967 Non-uniform propagation of imploding shocks and detonation. *A.I.A.A. J.* **5**, 1997–2003.

VON NEUMANN, J. 1941 The point source solution. *N.D.R.C., Div. B. Rep.* AM-9. (See also 1963 *John von Neumann Collected Works*, vol. VI (ed. A. H. Taub), pp. 219–237. Pergamon Press.)

OPPENHEIM, A. K., LUNDSTROM, E. A., KUHL, A. L. & KAMEL, M. M. 1971 A systematic exposition of the conservation equations for blast waves. *J. Appl. Mech.* **38**, 783–794.

ROGERS, M. H. 1958 Similarity flows behind strong shock waves. *Quart. J. Mech. Appl. Math.* **11**, 411–422.

SEDOV, L. I. 1945 On some non-steady-state motions of a compressible fluid. *Prikl. Mat. Mech.* **9**, 285–311.

SEDOV, L. I. 1946 Propagation of strong blast waves. *Prikl. Mat. Mech.* **10**, 241–250.

SEDOV, L. I. 1957 *Similarity and Dimensional Methods in Mechanics*, 4th edn. Moscow: Gostekhizdat. (Trans. 1959, ed. M. Holt. Academic.)

STANYUKOVICH, K. P. 1946 Application of particular solutions for equations of gas-dynamics to the study of blast and shock waves. *Rep. Acad. Sci. U.S.S.R.* **52**, 7.

STANYUKOVICH, K. P. 1955 *Unsteady Motion of Continuous Media.* Moscow: Gostekhizdat. (Transl. 1960, ed. M. Holt. Pergamon.)

TAYLOR, G. I. 1941 The formation of a blast wave by a very intense explosion. *British Rep.* RC-210. (See also 1950 *Proc. Roy. Soc.* A **201**, 175–186.)

TAYLOR, G. I. 1946 The air wave surrounding an expanding sphere. *Proc. Roy. Soc.* A **186**, 273–292.

WILSON, C. R. & TURCOTTE, D. L. 1970 Similarity solution for a spherical radiation-driven shock wave. *J. Fluid Mech.* **43**, 399–406.

ZEL'DOVICH, YA. B. & RAZIER, YU. P. 1966 *Physics of Shock Waves and High-Temperature Hydrodynamic Phenomena*, 2nd edn. p. 686. Moscow: Izdatel'stuo Nauka. (Trans. 1967, ed. W. D. Hayes & R. F. Probstein. Academic.)